Efficient Epidermis Segmentation for Whole Slide Skin Histopathological Images

Cheng Lu[1*] and Mrinal Mandal[2]

***Abstract*— In order to develop a computer-aided diagnosis system for histopathological skin cancer diagnosis, segmentation of the epidermis area is the very first and crucial step. An improved computer-aided epidermis segmentation technique for the whole slide skin histopathological image is proposed in this paper. The proposed technique first obtains an initial segmentation result with the help of global thresholding and shape analysis. A template matching method, with adaptive template intensity value, is then applied. Finally, a threshold is calculated based on the probability density function of the processed image after template matching. The threshold is then used to obtain the final segmentation result. Experimental results show that the proposed technique overcomes the limitation of the existing technique and provides a superior performance with sensitivity at 97.99%, and precision at 96.00%.**

I. Introduction

Histopathology slides provide a cellular-level view of diseased tissue, and is considered the "gold standard" in the diagnosis of most cancer diseases. However, the diagnostic decisions are subjective and often lead to intra-observer and inter-observer variability [1]. Also, the quantitative analysis of digitized whole slide image (WSI) is time-consuming and difficult. To address such limitations, computer-aided quantitative tools which can provide objective results are needed. Recently, researchers have applied sophisticated digital image analysis techniques to extract objective and accurate prognostic information throughout the WSI. For analyzing the breast cancer WSI, Roullier et al. [2] proposed a multi-resolution graph-based analysis framework that refines the segmentation result from lower to higher resolution layers. Wang et al. [3] developed an computer-aided diagnosis (CAD) system to classify the cervical intraepithelial neoplasia WSI based on different extracted features from the image appearance.

Skin melanoma is the most aggressive type of skin cancer [4]. Based on a recent article, about 70,000 people are diagnosed with melanoma every year, and around 9,000 die from it in the United States [5]. The early detection of malignant melanoma will help to lower the mortality rate. A normal skin tissue slide usually contains three main parts: epidermis area, dermis area and sebaceous tissues. When a pathologist examines a skin tissue, epidermis area is the first area to be examined since it provides critical information for most diseases. Therefore, the task of epidermis area segmentation is the very first and necessary step of a CAD system.

In terms of skin histopathological image analysis, Lu et al. proposed several image analysis techniques, which include the segmentation of epidermis area [6], and segmentation of keratinocytes [7] and melanocytes [8], [9]. In [6], Lu et al. utilized global threshold and shape analysis to segment the epidermis area in the red channel skin WSI. The technique provides a good performance in terms of sensitivity and specificity. However, the precision rate is relatively low since the segmentation result tends to include many false positive regions.

In this paper, we investigate the limitation of the epidermis segmentation technique discussed in reference [6], and propose an improved technique for automatic segmentation of the epidermis area in the skin WSI.

II. The Proposed Technique

The overall schematic of the proposed technique is shown in Fig. 1. The red channel image is used as the input since it provides the best discrimination between the dermis and epidermis [6]. The details of these modules are discussed below.

Fig. 1. The schematic of the proposed technique.

A. Initial Segmentation of Epidermis

In this module, an initial segmentation of epidermis is obtained using a global threshold and shape analysis method described in [6]. The basic idea is to first calculate a global threshold for the WSI and to segment the WSI while treating areas with lower value image as the foreground. The size and shape criteria are then applied to eliminate unrelated areas. We used the ratio between major and minor axes of best fit ellipse as the shape criterion since epidermis area is narrow and long object. We now obtain a binary image B which contains the initial segmentation result. Define the proportion of initial segmentation result as:

$$\mathbf{P}_{initial} = \frac{\mathcal{N}_e}{\mathcal{N}_a}. \quad (1)$$

where $\mathcal{N}_e$ is the number of pixels belonging to the initial segmentation and $\mathcal{N}_a$ is the number of pixels of the image

*This research is supported by the Fundamental Research Funds for the Central Universities of China (Grant NO.GK201402037)

[1]C. Lu is the corresponding author with College of Computer Science, Shaanxi Normal University, Xi'an Shaanxi Province 710119, China chenglu@snnu.edu.cn

[2]M. Mandal is with Electrical and Computer Engineering, University of Alberta, Edmonton, Alberta T6G 2V4, Canada mmandal@ualberta.ca

978-1-4244-7929-0/14/$26.00 ©2014 IEEE

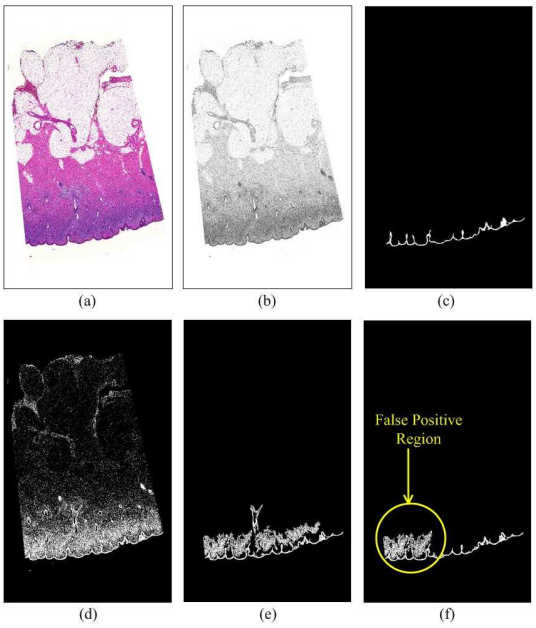

Fig. 2. An example of initial segmentation. (a) and (b) are the original color image and red channel image, respectively. (c) is the manually labeled binary image, where white region shows the epidermis area. (d) shows the binary image obtained after threshold. (e) shows the binary image obtained after applying size criterion. (f) shows the binary image obtained after applying the shape criterion, the false positive region is highlighted.

except the white background. $\mathbf{P}_{initial}$ will be used for latter processing.

After the initial segmentation, we can obtain a satisfactory epidermis area in most of the cases [6]. However, in other cases where the melanocytes invading into the dermis area, the appearance of the dermis and epidermis area are similar to each other (especially on the boundary between the dermis and epidermis areas). This will result in inaccurate segmentation result in which more false positive regions are included. An example is shown in Fig. 2. Fig 2.(a) and (b) show the original color image and red channel image, respectively. The manually labeled epidermis region is shown in Fig. 2(c), where white region represents the epidermis area. Fig. 2(d) shows the binary image obtained after global threshold. Note that because there are many melanocytes present in the dermis area. Once the threshold is applied, the segmented area contains many false positive regions (shown as white regions in Fig. 2(d)). Fig. 2(e) and (f) shows the binary image obtained after applying size criterion and shape criterion, respectively. Note that in Fig. 2(f), the initial segmentation result still contains false positive region (highlighted with circle) since the melanocyte regions in dermis are connected to the epidermis area.

B. Template Matching with Auto-generated Template

Template matching technique is a widely used technique for pattern detection in medical imaging [10], [11]. In the second module, we propose to apply a template matching (TM) technique to improve the segmentation performance, in which the template is generated automatically. The

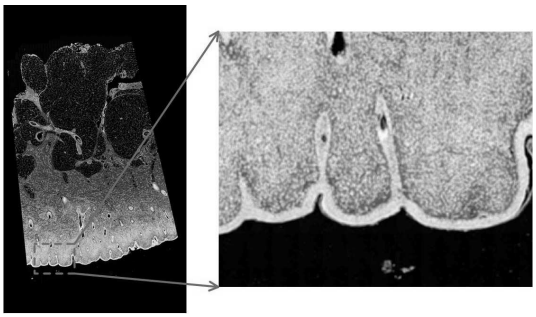

Fig. 3. An example of the response value image. The lower left portion of the image is zoomed in for more details. The higher response value corresponds to brighter level.

template is designed as a sub-portion of epidermis, and we assume that all the pixels belonged to epidermis have high response value after template matching and the epidermis area has homogenous intensity values than background.

Based on the initial segmentation result, a template is created for the template matching. The shape of the template is designed as a circle to ensure that the template can be included inside epidermis. The radius of the template is 3 pixels. The intensity of the template is adaptively chosen as the average intensity value of the initial segmentation result of epidermis (denote it as m).

In the TM implementation, the template is sliding on the red channel image, the response value is calculated by using the normalized cross correlation (NCC) [12], which is as follows:

a) Calculate zero mean image $I_Z(x, y)$, as follows:

$$I_Z(x, y) = I(x, y) - \overline{I}_{u,v} \tag{2}$$

where $I(x, y)$ is the pixel in the sub-image, (u, v) is the center of sub-image, $\overline{I}_{u,v}$ represents the mean of the sub-image.

b) Calculate the response value γ as follows:

$$\gamma(u, v) = \frac{\sum_{x,y} I_Z(x, y) t_Z(x - u, y - v)}{[\sum_{x,y} I_Z(x, y)^2 \cdot \sum_{x,y} t_Z(x - u, y - v)^2]^{1/2}} \tag{3}$$

$$t_Z(x - u, y - v) = t(x - u, y - v) - \bar{t} \tag{4}$$

where $t(x - u, y - v)$ is the pixel in the template, i.e., has value m, and $\bar{t}$ is the mean of template. For each position/pixel in the image, we will have a response value gamma, which is between 0 and 1. Intuitively, a high (low) response value indicates a higher (lower) probability that the current position/pixel belongs to epidermis. All these response values form an image, and henceforth we refer to this image as the response value image.

In the response value image, most pixels inside epidermis area have similar intensity values, and hence we can have homogenous high response value area. For the case that the melanocytes invading into the dermis area, the melanocytes may have high response values as well, however, the high response values are isolated and cannot form homogenous area. For all other areas, like blood vessel and gland in

dermis, which have different intensity value compared to the epidermis, will have lower response values. One example is shown in Fig. 3. It is shown that the epidermis area has homogenous high response value region. For the regions that have invading melanocytes we can observed many isolated high response value regions.

C. PDF Analysis

Once we obtain the response value image, we can now analysis the probability density function (PDF) of the response values in order to obtain a final global threshold for accurate epidermis segmentation.

In most cases of skin tissues, it has been observed that the PDF of the response value image has two modes: one is large and another one smaller. The larger mode corresponds to a large number of pixels belonging to unrelated regions that have lower response values. The smaller mode corresponds to the small number of pixels belonging to the epidermis region that have higher response values. Therefore, the local minimum value between the two modes can then be used for the final threshold for the response value image. Two examples are shown in Fig. 4. In the case where the melanocytes are not appeared in dermis area (shown in Fig. 4(a)), it is clear that the PDF has two modes. One is centered near the lower response value area (around 0.15) which correspond to the non-epidermis area, and another one is centered near higher response value area (around 0.5) which correspond to the epidermis area. The minimum is highlighted in the bottom image of Fig. 4(a), the corresponding response value can be chosen as the threshold for segmentation. In the case where too many melanocytes are present in the dermis area (shown in Fig. 4(b)), the PDF is not bi-modes. As there are many melanocytes presented in the dermis area, we have relatively large number of high response values. Therefore, we can only observe one peak near the lower response value area.

Assume that the discrete response value are sampled with a step of 0.02. Then we have $\delta \in [0, 0.02, 0.04, \ldots, 0.98, 1]$, where δ is a random variable. The probability of δ is defined as $P(\delta)$. Based on the characteristics of the PDF, we propose the following strategy to find the final threshold for the response value image segmentation:

1) Analyze if the PDF is bi-modal.

2) If the PDF is bi-modal, the minimum $P(\delta^*)$ between the two modes will be located and the corresponding response value δ^* will be used as the threshold.

3) If the PDF is not bi-modal, the threshold δ^* will be calculated such that it satisfies the following equation:

$$\sum_{\delta=0}^{\delta^*} P(\delta) = 1 - \mathbf{P}_{initial} \tag{5}$$

Eq. 5 indicates that we are calculating the main component of the PDF from the lower value area (specifically from value 0). Since it is difficult to find the threshold, we utilize the initial segmented epidermis area proportion from Eq. 1 to find the threshold. In other words, the threshold for current response value image will be the lower bound to calculate the accumulative probability function that reaches $1 - \mathbf{P}_{initial}$.

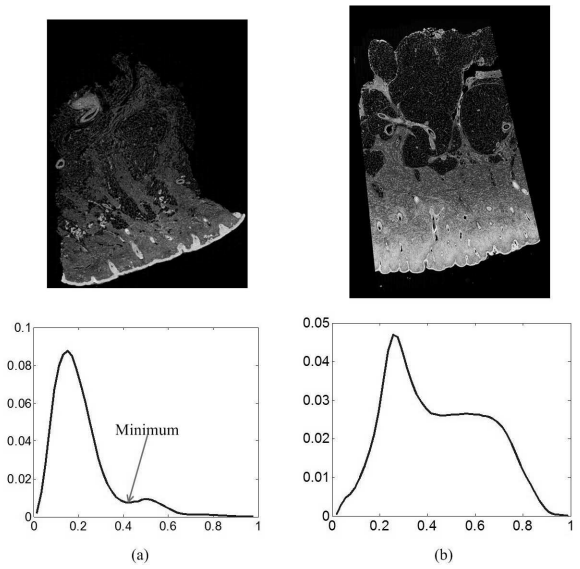

Fig. 4. Two examples of PDF of the response value image. (a) shows the case where the melanocytes are not present in dermis area. The response value image is shown on the top and its corresponding PDF is shown at the bottom. (b) shows the case where the melanocytes are found in dermis area.

Once we obtain the threshold δ^*, the response value image will be segmented. The pixels in epidermis area has high response values, and therefore the pixels greater than the threshold δ^* will be treated as epidermis area, and other pixels are treated as background. After the segmentation of response value image, the size and shape criterion, described in [6], are then applied again to obtain the final epidermis. Finally, the morphological opening operation with disk-like structure is applied to obtain the final segmentation result.

III. Performance Evaluation

We have evaluated the proposed technique on 62 different skin WSIs. The histological sections used for image acquisition are prepared from formalin-fixed paraffin-embedded tissue blocks of skin biopsies. The sections prepared are about 4μm thick and are stained with H&E using automated stainer. These images are captured under 40X magnification (0.24 μm/pixel) on Carl Zeiss MIRAX MIDI Scanning system (Carl Zeiss Inc., Germany). All test images are down sampled with a factor of 32. After the down sampling, all of the test image are between 2500×3000 to 6000×10000 pixels.

The manually labeled pixel-level contour of the epidermis, by expert, is treated as the ground truths for evaluation. For the evaluation metric computation, we define GT as the ground truth region, SEG as the segmented region obtained by the automated technique. Three area-based evaluation metrics: sensitivity ($\mathcal{A}_{SEN}$), specificity ($\mathcal{A}_{SPE}$), precision ($\mathcal{A}_{PRE}$) are defined as follows:

$$\mathcal{A}_{SEN} = \frac{|GT \bigcap SEG|}{|GT|} \times 100\% \tag{6}$$

TABLE I

PERFORMANCE EVALUATION OF THE EPIDERMIS SEGMENTATION.

	$\mathcal{A}_{SEN}$	$\mathcal{A}_{SPE}$	$\mathcal{A}_{PRE}$
GTSA	97.24%	98.14%	62.84%
Proposed Tech.	97.99%	99.60%	96.00%

$$\mathcal{A}_{SPE} = \frac{|\overline{GT} \bigcap \overline{SEG}|}{|\overline{GT}|} \times 100\% \quad (7)$$

$$\mathcal{A}_{PRE} = \frac{|GT \bigcap SEG|}{|SEG|} \times 100\% \quad (8)$$

where $|\cdot|$ is the cardinality operator. We also compared the segmentation result with the technique proposed in reference [6], and we refer this technique as GTSA (global threshold and shape analysis) technique henceforth.

The performance of the two epidermis segmentation techniques on red channel images for 62 test WSIs are shown in Table I. The first column shows the name of technique for segmentation of epidermis. The second to the fourth columns show the area-based sensitivity, specificity and precision, respectively. It is observed that in terms of sensitivity, the GTSA and the proposed techniques provide similar result (97.24% compared to 97.99%). It indicates that both techniques are able to segment most of the epidermis area successfully. However, in terms of the precision rate, the GTSA technique is at 62.84%. In other words, the segmentation result obtained by the GTSA technique contains many false positive area which are not the true epidermis area. On the other hand, the proposed technique is able to eliminate the false positive areas and provides 96% precision rate, which outperforms the GTSA technique. Fig. 5 show examples of the final segmentation results obtained by the GTSA and the proposed technique. It is observed that the GTSA technique tend to include more false positive regions near the epidermis. The result obtained by the proposed technique is very close to the ground truth data. Overall, the proposed technique is able to provide a satisfactory segmentation result on the 62 WSIs dataset.

IV. CONCLUSIONS

This paper presents an improved technique for epidermis segmentation in skin WSI. Based on the initial segmentation result, a template matching method is applied on the red channel image to enhance the signal of epidermis. A final threshold is determined to obtain the epidermis segmentation. The proposed technique addresses the limitation of the existing technique and provides superior performance in the evaluation. Further quantitative analysis, e.g., melanocytes detection in the epidermis, is able to perform based on this work.

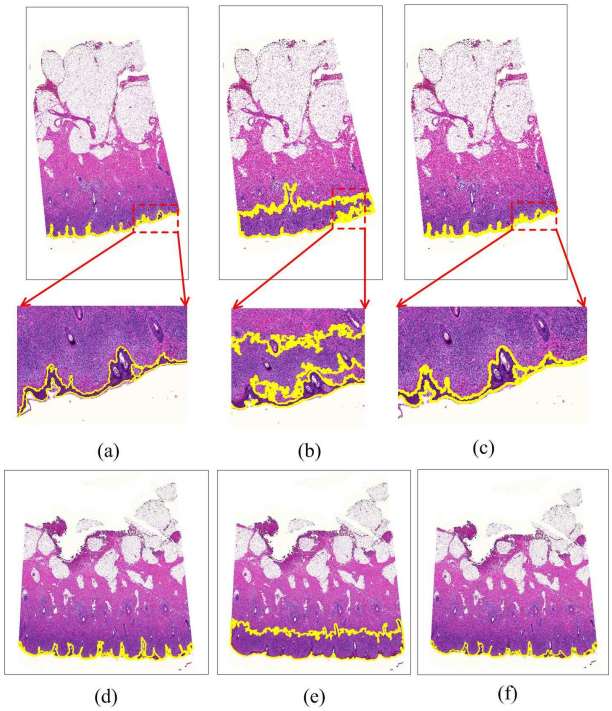

Fig. 5. Examples of the final segmentation results. The epidermis area contours are superimpose on the original images. (a) and (d) show the segmentation result obtain by the proposed technique. (b) and (e) show the segmentation result obtain by the GTSA technique. (c) and (f) show the manually labeled epidermis contours.

REFERENCES

[1] S. Ismail, A. Colclough, J. Dinnen, D. Eakins, D. Evans, E. Gradwell, J. O'Sullivan, J. Summerell, and R. Newcombe, "Observer variation in histopathological diagnosis and grading of cervical intraepithelial neoplasia." *British Medical Journal*, vol. 298, no. 6675, p. 707, 1989.

[2] V. Roullier, O. Lezoray, V. Ta, and A. Elmoataz, "Multi-resolution graph-based analysis of histopathological whole slide images: Application to mitotic cell extraction and visualization," *Computer medical imaging and graph*, 2011.

[3] Y. Wang, D. Crookes, O. S. Eldin, S. Wang, P. Hamilton, and J. Diamond, "Assisted diagnosis of cervical intraepithelial neoplasia (cin)," *IEEE Journal of Selected Topics in Signal Processing*, vol. 3, no. 1, pp. 112–121, 2009.

[4] I. Maglogiannis and C. Doukas, "Overview of advanced computer vision systems for skin lesions characterization," *IEEE Transactions on Information Technology in Biomedicine*, vol. 13, no. 5, pp. 721–733, 2009.

[5] American Cancer Society, "What are the key statistics about melanoma?" American Cancer Society, Tech. Rep., 2008.

[6] C. Lu and M. Mandal, "Automated segmentation and analysis of the epidermis area in skin histopathological images," in *2012 Annual International Conference of the IEEE Engineering in Medicine and Biology Society (EMBC)*, 2012, pp. 5355–5359.

[7] C. Lu, M. Mahmood, N. Jha, and M. Mandal., "A robust automatic nuclei segmentation technique for quantitative histopathological image analysis," *Analytical and Quantitative Cytology and Histopathology*, vol. Vol. 12, pp. 296–308, 2012.

[8] C. Lu, M. Mahmood, N. Jha, and M. Mandal, "Detection of melanocytes in skin histopathological images using radial line scanning," *Pattern Recognition*, vol. Volume 46, Issue 2, pp. 509–518, 2013.

[9] ——, "Automated segmentation of the melanocytes in skin histopathological images." *IEEE Journal of Biomedical and Health Informatics*, vol. Vol. 17, pp. 284–296, 2013.

[10] S. Naik, S. Doyle, S. Agner, A. Madabhushi, M. Feldman, and J. Tomaszewski, "Automated gland and nuclei segmentation for grading of prostate and breast cancer histopathology," in *Proc. 5th IEEE Int. Symp. Biomedical Imaging: From Nano to Macro ISBI 2008*, 2008, pp. 284–287.

[11] I. Sintorn, M. Homman-Loudiyi, C. Söderberg-Nauclér, and G. Borgefors, "A refined circular template matching method for classification of human cytomegalovirus capsids in tem images," *Computer methods and programs in biomedicine*, vol. 76, no. 2, pp. 95–102, 2004.

[12] J. Lewis, "Fast normalized cross-correlation," in *Vision Interface*, vol. 10. Citeseer, 1995, pp. 120–123.